FDG Uptake, GLUT-1 Glucose Transporter and Cellularity in Human Pancreatic Tumors

Tatsuya Higashi, Nagara Tamaki, Tatsuo Torizuka, Yuji Nakamoto, Harumi Sakahara, Toshiyuki Kimura, Toyohiko Honda, Tetsuro Inokuma, Shinji Katsushima, Gakuji Ohshio, Masayuki Imamura and Junji Konishi

Department of Nuclear Medicine and First Department of Surgery, Kyoto University Faculty of Medicine, Kyoto; and Hokkaido University School of Medicine, Sapporo, Japan

We previously reported that grading of GLUT-1 glucose transporter expression was related closely to FDG accumulation in FDG PET in human cancers. But in this strong GLUT-1 expression group, there was an enormous range of standardized uptake values (SUVs) within them. **Methods:** To evaluate other factors determining the FDG PET uptake, FDG PET was performed in 36 preoperative patients (mean age 62.0 yr) suspected of having pancreatic tumors, including 33 malignant and 3 benign neoplastic tumors. FDG uptake at 50 min after injection of 185 MBq ^{18}F-FDG with > 5 hr fasting condition was semiquantitatively analyzed as SUVs. The GLUT-1 expression was studied by immunohistochemistry of paraffin sections from these tumors after the operation using the antiGLUT-1 antibody. The number of tumor cells within a 5- × 5-mm square was counted manually using ×200 magnification photographs and was graded immunohistochemically as strong, weak or negative. **Results:** In all 36 cases there were 3 cases of GLUT-1 negative, 8 of GLUT-1 weak positive and 25 of GLUT-1 strong positive. In all cases, the total number of tumor cells had no significant value for SUVs. Among 33 GLUT-1 positive cases, the number of GLUT-1 positive tumor cells correlated significantly with SUVs ($p < 0.01$). Only in 25 strong grade cases, the number of GLUT-1 strong positive tumor cells had a more significant value for SUVs ($p < 0.005$). Computational multivariate analysis using multiple regression for SUVs was performed evaluating the five variables as follows: tumor size, GLUT-1 immunohistochemical grading, number of total tumor cells, number of total GLUT-1 positive tumor cells and number of GLUT-1 strong positive cells. This analysis revealed that only the variable, the number of GLUT-1 strong positive cells, had a significant regression coefficient for SUVs (standard regression coefficient = 0.855, $p < 0.0001$). **Conclusion:** These data indicate that GLUT-1 expression plays an essential role in higher FDG accumulation in pancreatic tumor FDG PET, and the cellularity has a significant influence on SUVs only in the condition of GLUT-1 strong positive expression.

Key Words: pancreatic tumor; GLUT-1 expression; fluorodeoxyglucose PET; immunohistochemistry; cellularity

J Nucl Med 1998; 39:1727–1735

PET with ^{18}F-labeled fluorodeoxyglucose (FDG) has shown promise in oncological imaging. An increase in FDG uptake has been demonstrated in a variety of malignant tumors (*1–8*). For pancreatic tumors, we have reported the clinical values of FDG PET for detecting and differentiating pancreatic carcinoma (*9,10*).

The FDG accumulation is presumed to be due to enhanced exogenous glucose utilization in the tumor area (*11*). This theory is based on the observation of Warburg that malignant tumors are characterized by increased glucose metabolism compared with healthy cells (*12*). In immunohistochemical study of human pancreatic cancers, we recently reported the close relationship between FDG accumulation in FDG PET and the grading of immunohistochemical expression of GLUT-1 glucose transporter in the resected tumor tissues. However, in the strong GLUT-1 expression group, there was an enormous range of SUVs within them. There was no reported relationship between FDG and other glucose transporters: GLUT-2, 3, 4 and 5 (*13*).

Recent in vitro study showed that FDG accumulation has a close relationship with the number of viable tumor cells rather than with proliferative activity (*14*). Some studies showed that not only tumor cells, but fibrous tissue or inflammatory cells, could have some weak accumulation of FDG (*15–18*). Furthermore, some clinical studies showed that the size of the scanned tumor had some influence on the result of maximal SUV in FDG PET (*19,20*). Many complicated factors are supposed to affect the results of FDG accumulation in clinical FDG PET imaging. But no correlative study has been reported so far about the relationship among tumor size, FDG accumulation, the number of tumor cells and immunohistochemical expression of GLUT-1 glucose transporter in the resected human tumor tissues.

In this study, to evaluate other factors determining FDG PET uptake, we performed a series of FDG PET studies and, after surgery, examined tumor size and the number of tumor cells and the immunohistochemical expression of the GLUT-1 glucose transporter in the resected pancreatic tumor tissue specimen.

MATERIALS AND METHODS

Patients

The study group consisted of 36 patients with suspected pancreatic tumors (18 men, 18 women; age range 19–81 yr; mean age 60.9 yr) examined between June 1992 and June 1996 who had surgery. Pancreatic tumors were suspected on the basis of clinical findings, laboratory data, ultrasound and CT results. Patients had preoperative imaging with FDG PET within 1–3 wk before surgery. They all had surgery and proved to have neoplastic tumors. All paraffin sections were obtained from their resected tumors.

In all 36 patients a histological diagnosis was made after surgery that found 24 patients had ductal adenocarcinoma, 4 had mucinous cystadenocarcinoma, 3 had ampullary carcinoma, 2 had islet cell tumors, 2 had mucinous cystadenoma and 1 had solid and cystic tumors.

Before being enrolled in this study, each patient gave written informed consent, as required by the Kyoto University Human Study Committee.

PET Imaging

All the PET imaging procedures in this study were exactly the same as in our previous article (*13*).

Received May 23, 1997; revision accepted Jan. 14, 1998.

For correspondence or reprints contact: Tatsuya Higashi, MD, Department of Nuclear Medicine, Kyoto University Faculty of Medicine, Shogoin, Sakyo-ku, Kyoto, 606-01 Japan.

Imaging Technique

Fluorine-18 was produced by ^{20}Ne (d, α) ^{18}F nuclear reaction, and ^{18}F-labeled FDG was synthesized with the acetyl hydrofluorite method (*21*). PET was performed with a whole-body PET camera (PCT3600W; Hitachi Medico, Tokyo, Japan) with eight rings, which provides 15 tomographic sections at 7-mm intervals. The intrinsic resolution was 4.6 mm FWHM at the center, and the axial resolution was 7 mm FWHM. The effective resolution after reconstruction was approximately 10 mm. The field of view and the pixel size of the reconstructed images were 512 mm and 4 mm, respectively. Scatter correction was not performed.

The patients fasted for at least 5 hr before the FDG injection. Before the time of imaging, the exact position of pancreatic tumors was certified and marked by ultrasound sonography. The patient was positioned on the PET camera bed and underwent transmission scanning for attenuation correction in image reconstruction for 20 min. After the transmission scan, approximately 150–250 MBq (4.1–6.8 mCi) FDG were administered intravenously. About 50–55 min later, the patient was repositioned exactly the same as the transmission position on the PET camera bed according to position markings. Exactly 60 min after the FDG injection, static scanning was performed for 15 min (*9*).

Image Analysis

PET images were compared with the corresponding CT images for accurate identification of the tumor by anatomical landmarks (for example, the upper and lower part of the kidney, the shape of the liver and the gallbladder bed). FDG accumulation was analyzed quantitatively by calculating the standardized uptake value (SUV) in the ROIs (regions of interest) placed over the tumor, the normal pancreas and the normal liver (*22*) as follows:

$$SUV = \frac{\text{PET count} \times \text{Calibration factor (mCi/g)}}{\text{Injection dose (mCi)/Body weight (g)}}$$

The ROI placed over the tumor was 10 × 10 mm (independent of tumor size), and it was placed in areas of the tumor that showed the highest FDG activity (*9*). The ROIs placed over the normal pancreas and the normal liver were 10 × 10 mm and 25 × 25 mm, respectively (*9*).

Histological Examination

Each section from each tumor was resected in the middle of the tumor area and had enough size of more than 1 cm in diameter of tumor tissue area. All sections were processed in paraffin for routine pathology.

Immunohistochemical Procedure

All the immunohistochemical procedures in this study were exactly the same as our previous article (*13*).

The polyclonal rabbit antiglucose transporter antibody reactive with GLUT-1 (rat) (brain/erythrocyte type) (East Acre Biological, Southbridge, MA) was raised against synthetic peptide (13-mer) based on the deduced amino acid sequence of the carboxy terminus of the rat brain glucose transporter (CGLFHPLGADSQV). It immunoreacts with a 50,000-Dalton glucose transporter species in rat brain and human erythrocytes and cross-reacts with the human hepatocarcinoma cells' (HEP G2) glucose transporter. It was diluted 1:1000 with 0.05 *M* Tris-HCl buffer, pH 7.5, containing 1% bovine serum albumin (Sigma, St. Louis, MO).

Paraffin sections from each tumor were deparaffinized with xylene and ethanol and unmasked with target unmasking fluid (TUF) (MONOSAN, Uden, The Netherlands). Then the sections were washed with PBS for 15 min (3 times, 5 min each time) and blocked for 30 min at 25°C with 10% normal bovine serum in PBS (DAKO, Carpinteria, CA). Then, the sections were incubated with the antiGLUT-1 glucose transporter antibody as the primary antibody for 1 hr at 25°C. Parallel sections were incubated with healthy rabbit immunoglobulin G (Ig G) (2 μg/ml, 20 μg/ml) as negative controls. Then, the sections were washed with PBS for 15 min (3 times, 5 min each time). In the following steps each section was stained by the labeled streptavidin-biotin method using the DAKO LSAB kit. For linking, the sections were incubated with the second antibody for 10 min at 25°C and washed with PBS for 15 min. Then, they were incubated with streptavidin peroxidase and washed with PBS for 15 min. Being substituted for AEC Chromogen, 3,3′-diaminobenzidine tetrahydrochloride (DAB) (DAKO), was used as substrate-chromogen solution at 25°C for 10 min, diluted in 1 mg/ml with 0.05 *M* Tris-HCl buffer, pH 7.5. Then the sections were rinsed gently with distilled water and washed in

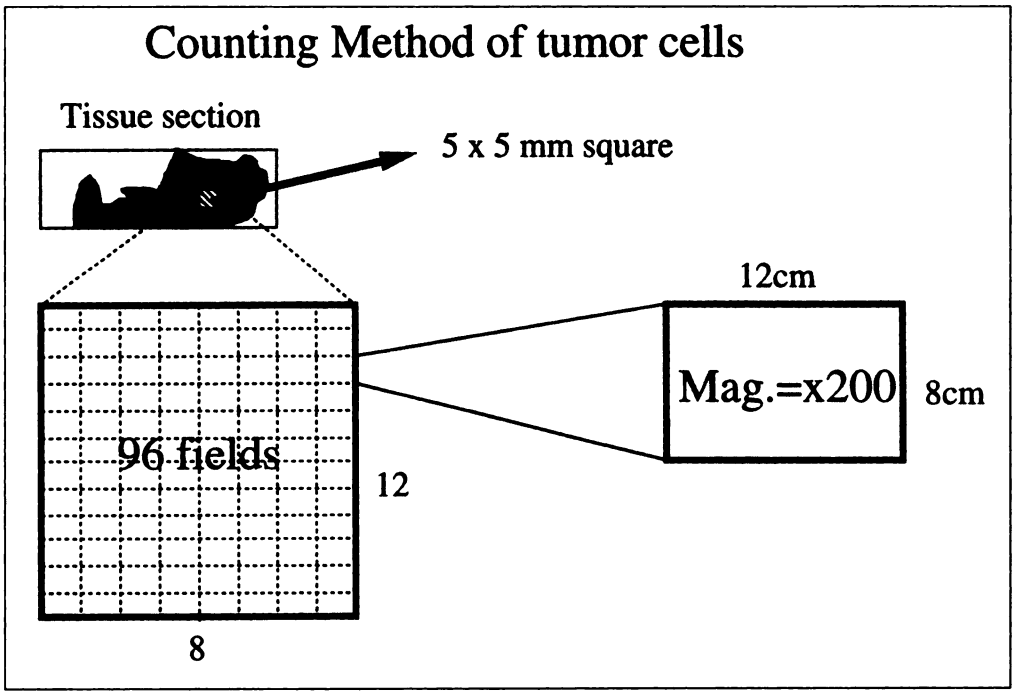

FIGURE 1. Schematic figure for counting method of number of tumor cells. Photographic cuts of 12 × 8 = 96 were taken in each 5- × 5-mm square of tissue section of tumor. Magnification of photographs was ×200.

flowing water for 15 min. In the last step, the sections were lightly counterstained with Mayer's hematoxylin and then dehydrated, dealcoholized and coverslipped with mounting media. Other chemicals not mentioned above were of reagent grade or of the highest purity available.

For positive controls, normal tissues from the appropriate pancreatic and duodenal areas were available. We also used as positive controls, the DAKO control slides (checkerboard normal multitissue block and checkerboard multitumor block). All slides were examined by light microscopy.

Immunohistochemical Grading

Immunohistochemical grading was performed by three independent, experienced physicians without the information of SUVs for each tumor cell.

Counting Method of the Number of Tumor Cells

For the tumor cell counting in this study, a modified method based on the original report of Wang et al. (*23*) was performed. Each processed section from each tumor was photographed in the square region of 5 × 5 mm near the center of the tumor area. The magnification was ×200, and each printed photograph was 8 × 12 cm in size. Therefore, every tumor had 96 photographic cuts (Fig. 1).

For each patient, the total number of tumor cells was examined four times and manually counted by three experienced physicians. In two counts, all 96 photographic cuts were examined. In the other two counts, a random selection of 10 photographic cuts was examined, and each result was multiplied by 10. In each photograph, the percentages between the GLUT-1 negative, weak positive and strong positive tumor cells also were examined. Our results of the tumor cells in this study were shown as an average of these four examinations.

Statistical Analysis

The data presented in this paper were expressed as mean ± s.d. Probability values of less than 0.05 indicated a statistically significant difference. The nonparametric statistical analysis between each counting result and that between the SUVs and the number of tumor cells were performed by analysis of variance followed by the Spearmann rank collection test. The computational multivariate analysis was performed by multiple regression analysis using the software Statistica (Stat Soft, Inc., Tulsa, OK).

TABLE 1
Results of FDG PET Imaging, Cellularity and Immunoreactivity of GLUT-1 Glucose Transporter in 36 Pancreatic Tumors

			Tumor characteristics			FDG PET diagnosis				
Patient	Age (yr)	Sex	Histological diagnosis	Size (mm)	Stage*		Standardized uptake value	GLUT-1 grading	Number of total tumor cells average ± s.d.	
					Malignant lesions (n = 33)					
1	65	M	Ductal adenocarcinoma	28	T2N1M0	Malignant	2.52	Negative	17826	±6314
2	63	M	Ductal adenocarcinoma	30	T2N0M0	Malignant	2.80	Negative	18656	4099
3	72	M	Ductal adenocarcinoma	60	T3N1M1	Malignant	2.87	Negative	40939	1453
4	62	M	Cystadenocarcinoma	10	T1aN0M0	False-negative	2.04	Weak	16057	17548
5	57	F	Islet cell tumor	45		Malignant	2.44	Weak	62631	3407
6	77	M	Cystadenocarcinoma	30	T1bN0M0	Malignant	2.50	Weak	22808	2480
7	71	F	Ductal adenocarcinoma	18	T1aN0M0	Malignant	2.74	Weak	11458	5192
8	55	M	Ductal adenocarcinoma	40	T3N1M0	Malignant	3.62	Weak	71821	6102
9	59	F	Ductal adenocarcinoma	50	T2N1M1	Malignant	3.88	Weak	8185	1413
10	64	F	Ductal adenocarcinoma	80	T3N1M1	Malignant	4.67	Weak	27519	2035
11	55	F	Ductal adenocarcinoma	30	T1bN1M0	Malignant	5.49	Weak	12675	1120
12	77	M	Cystadenocarcinoma	28	T1bN0M0	False-negative	1.76	Strong	3213	698
13	63	F	Ampullary carcinoma	16	T1aN0M0	Malignant	2.62	Strong	41468	1977
14	69	F	Ampullary carcinoma	15	T2N0M0	Malignant	2.78	Strong	5890	1724
15	45	M	Cystadenocarcinoma	70	T2N0M0	Malignant	2.88	Strong	17388	7232
16	62	F	Ductal adenocarcinoma	28	T3N1M0	Malignant	2.91	Strong	16869	2014
17	67	F	Ductal adenocarcinoma	20	T1bN1M0	Malignant	3.09	Strong	21578	6963
18	68	F	Ductal adenocarcinoma	50	T3N1M0	Malignant	3.17	Strong	3924	574
19	79	M	Ductal adenocarcinoma	30	T3N0M0	Malignant	3.28	Strong	7430	1494
20	76	F	Ductal adenocarcinoma	70	T3N1M1	Malignant	3.49	Strong	8975	3256
21	51	M	Ductal adenocarcinoma	25	T2N0M0	Malignant	3.55	Strong	12901	1342
22	52	M	Ductal adenocarcinoma	40	T3N1M0	Malignant	3.71	Strong	15130	5380
23	58	M	Ductal adenocarcinoma	50	T3N1M1	Malignant	4.19	Strong	24580	4229
24	81	M	Ductal adenocarcinoma	50	T3N1M1	Malignant	4.84	Strong	9418	1960
25	67	F	Ductal adenocarcinoma	80	T3N1M1	Malignant	4.84	Strong	24558	2221
26	69	M	Ductal adenocarcinoma	70	T3N1M1	Malignant	5.58	Strong	53250	5967
27	69	M	Ductal adenocarcinoma	80	T3N1M1	Malignant	5.71	Strong	17410	2134
28	66	M	Ductal adenocarcinoma	70	T3N1M1	Malignant	5.93	Strong	13357	2756
29	66	M	Ductal adenocarcinoma	70	T3N1M0	Malignant	5.98	Strong	14204	2769
30	55	F	Ductal adenocarcinoma	55	T3N1M1	Malignant	6.27	Strong	5711	1688
31	46	M	Ductal adenocarcinoma	70	T3N1M1	Malignant	6.90	Strong	31189	6437
32	61	F	Islet cell tumor	60		Malignant	15.12	Strong	36860	1750
33	61	F	Ampullary carcinoma	35	T3N1M1	Malignant	16.35	Strong	84217	5814
					Benign lesions (n = 3)					
34	46	F	Cystadenoma	40		Benign	1.31	Strong	1046	246
35	65	F	Cystadenoma	30		Benign	1.94	Strong	1597	527
36	19	F	Solid and cystic tumor	35		False-positive	3.9	Strong	59996	17310

*Tumor stage according to reference 32.

TABLE 2
Comparison Between Standardized Uptake Values (SUVs) and Total Tumor Cell Cellularity in Each Histology

Tumor diagnosis	n =	SUV/average ± s.d.	SUV min.–max.	Number of total cells/ average ± s.d.	×0.00019
Malignant lesions	33	4.56 ± 3.18		23,639 ± 19,773	4.49 ± 3.76
Ductal adenocarcinoma	24	4.25 ± 1.31	2.52–6.9	20,398 ± 15,807	3.88 ± 3.00
Cystadenocarcinoma	4	2.30 ± 0.50	1.76–2.88	14,867 ± 8,300	2.82 ± 1.58
Ampullary carcinoma	3	7.25 ± 7.88	2.62–16.35	43,858 ± 39,218	8.33 ± 7.45
Islet cell tumor	2	8.78 ± 9.00	2.44–15.12	49,746 ± 18,223	9.45 ± 3.46
Benign lesions	3	2.38 ± 1.35		20,880 ± 33,877	3.97 ± 6.44
Cystadenoma	2	1.63 ± 0.45	1.31–1.94	1,322 ± 390	0.25 ± 0.07
Solid and cystic tumor	1	3.9		59,996	11.40
Normal pancreas	36	1.60 ± 0.47			
Normal liver	36	2.26 ± 0.38			

RESULTS

Table 1 summarizes the tumor characteristics, the results of FDG PET imaging and the immunohistochemical findings of the 36 patients studied. The results of SUVs and the total tumor cell cellularity in each histological diagnosis are shown in Table 2.

PET Imaging Diagnosis

The histological examination showed that 33 of 36 tumors were malignant and 3 were benign (Table 1). In the quantitative analysis of FDG PET uptake, the SUVs of malignant tumors ranged from 1.76 to 16.35 with the mean value of 4.56 ± 3.18, which were higher than those of benign lesions (range 1.31–3.9; mean value 2.38 ± 1.35) (Table 2).

Immunohistochemical Grading of GLUT-1

Negative control sections showed no staining with healthy rabbit immunoglobulin G (Ig G) (2 μg/ml, 20 μg/ml). The results of the grading by the three physicians were concordant in all the patients. The interobserver variance in our grading was 0/36 (0%).

Of 33 malignant tumors proved by histological examination, 30 tumors (91%) showed positive for expression of GLUT-1 glucose transporter, and 22 (67%) showed strong (Table 1) (Fig. 2A-D, F). Only 3 patients (9%) with ductal adenocarcinoma did not show the GLUT-1 immunoreactivity. The three benign tumors had strong GLUT-1 expression (Fig. 2E).

Tumor Cell Counting in Each GLUT-1 Grading

The results of the four counts by the three physicians are shown in Table 3. Each standard deviation of each grading in each patient was compared with 20% and 30% of the average of each of them. The intraobserver and interobserver errors were 72 of 144 (50%) and 41 of 144 (29%), respectively. The intraobserver and interobserver variances also are shown in Table 4 as the multiple regression coefficient of determination. The intraobserver errors between the first and the second examinations done by the same physician were low (R-squares were more than 0.992). In the group of strong and total cells, the tumor cell cellularity was not statistically significant or was the same as that between each observer (R-squares were more than 0.894). Relatively wider interobserver variances were observed between the grades of negative and weak, especially in the counting by the second physician.

Correlation Between Standardized Uptake Values, Cellularity and GLUT-1 Expression

Mean value of SUVs in each grading case was calculated as follows: strong (n = 25) 4.9 ± 3.6, weak (n = 8) 3.4 ± 1.2 and negative (n = 3) 2.7 ± 0.2. SUVs increased in relation to the grade of GLUT-1 immunoreactivity, but there was no significant difference among them in this study. There also were no significant differences among mean values of the total number of tumor cells in the three grading groups (strong 21286 ± 20321, weak 29144 ± 24437 and negative 25807 ± 13111).

The nonparametric statistical analysis showed a statistically significant correlation between SUVs and the number of GLUT-1 strong positive cells among the 25 strong positive cases (R square = 0.695, $p < 0.005$) (Fig. 3). The same correlation was observed between SUVs and the number of GLUT-1 positive cells in the 33 strong and weak positive cases (R square = 0.441, $p < 0.01$). But there was no significant relationship between SUVs and the total number of tumor cells in all 36 cases studied.

Multivariate Analysis

Five variances of the multivariate analysis for SUVs were selected as shown in Table 5. The analysis revealed the multiple regression equation for SUVs as: SUVs = 4.1790 + 0.00019× (the number of GLUT-1 strong positive tumor cells) + 0.02642× (tumor size/mm) − 1.1009× (GLUT-1 grading) − 0.52124× (the number of total tumor cell) + 0.0002× (the number of GLUT-1 positive tumor cell).

$$\text{F value} = 14.77 > F_{(5,30)}(0.005) = 4.2276.\ R^2 = 0.71112.$$

Each regression coefficient also is shown in Table 5. The variance, the number of GLUT-1 strong positive tumor cells, was significant only for SUVs (standard regression coefficient; beta = 0.855, p = 0.0013). Tumor size was a weak factor for SUVs (beta = 0.175, p = 0.0931, not significant). The variance, the grading of GLUT-1 immunoreactivity, had a minus and weak value of regression coefficient (beta = −0.227, p = 0.1012, not significant).

To confirm our analysis, two patients (Patients 8 and 33) were eliminated from multivariate analysis because of the widest residuals calculated as Mahalanobis generalized distance (*24*). In these 34 patients almost the same results were obtained (Table 5).

Comparison Between Standardized Uptake Values and Cellularity in Each Histology

Table 2 shows the close relationship between SUVs and the 0.00019 divided number of total tumor cells (0.00019; regression coefficient of the number of GLUT-1 strong positive tumor cells) as shown in Table 5. There is supposed to be a close relationship between SUVs and the tumor cell

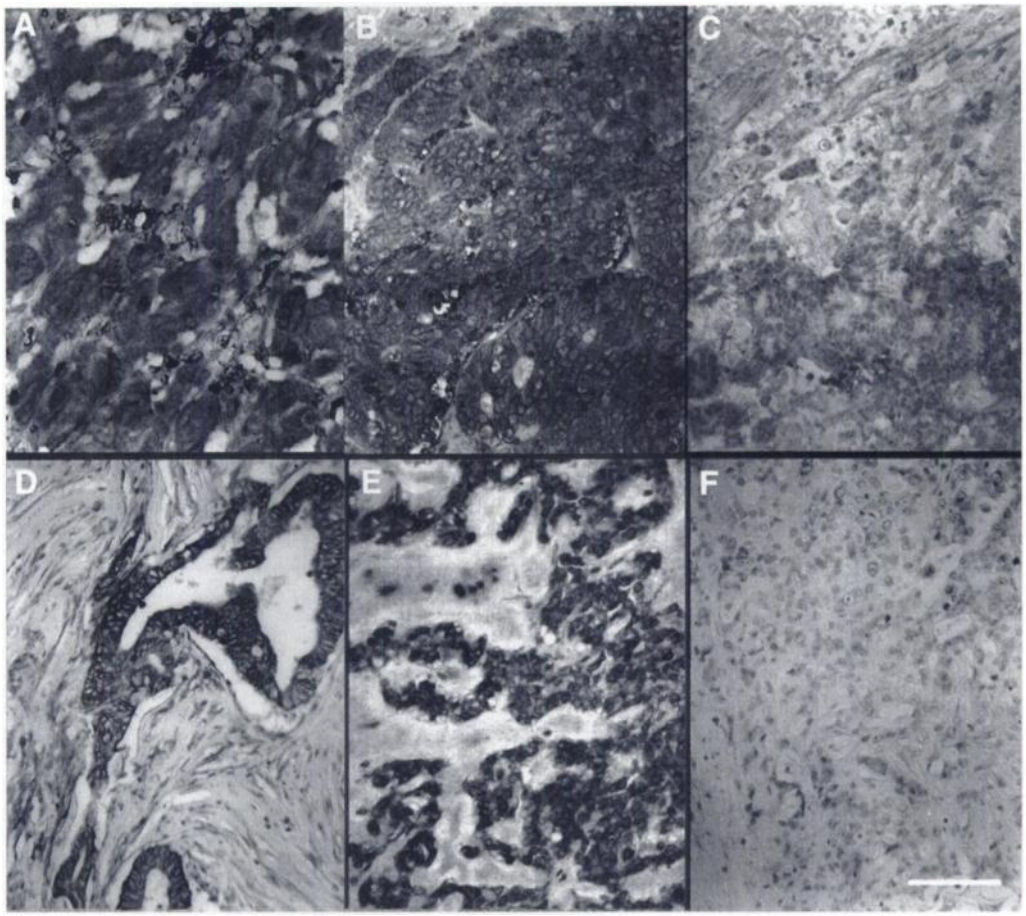

FIGURE 2. Examples of negative and strong expressions of GLUT-1 glucose transporter in sections of human pancreatic tumors immunostained with antiGLUT-1 and counterstained with Mayer's hematoxylin. Magnification is ×150 and Bar = 100 μm. (A) Patient 32, islet cell tumor. In almost the entire tumor area, tumor cells showed strong and homogeneous GLUT-1 expression with dense tumor cell cellularity. (B, C) Patient 26, ductal adenocarcinoma. Heterogeneity of GLUT-1 expression was observed. Some areas showed massive, strong positive GLUT-1 expression (B), while another area showed GLUT-1 negative (C). (D) Patient 16, ductal adenocarcinoma. Desmoplastic change of a ductal adenocarcinoma. Malignant ductlike structures with strong GLUT-1 expression are located within fibrous stroma. (E) Patient 36, solid and cystic tumor. Pseudopapillary structure with tumor cells and necrosis. (F) Patient 1, ductal adenocarcinoma. Ductlike structure was rare and all tumor cells were GLUT-1 negative.

cellularity in each histological type, especially in malignant tumor cases.

Normal Tissues and Positive Controls

Normal tissues and positive controls were stained almost the same as in our previous article (*13*).

DISCUSSION

Our data show a close correlation among tumor cell cellularity, immunoreactivity of GLUT-1 and SUVs in FDG PET, while also showing that there were only a few correlations between each of them alone. On the other hand, the multivariate analysis revealed that the number of GLUT-1 strong positive tumor cells was the most significant factor for SUVs. These findings suggest that only in the conditions of both higher tumor cell cellularity and increased expression of GLUT-1 transporter altogether, pancreas tumors can have a higher rate of entry of the FDG into the tumor cells. In other words, GLUT-1 expression was supposed to play an essential role in higher FDG accumulation in pancreatic tumor FDG PET, and only in the condition of GLUT-1 strong positive expression was the cellularity supposed to have a significant value on SUVs.

Fluorine-18-fluorodeoxyglucose (FDG) is now used widely as a tracer for the study of glucose metabolism in various organs and tumors. We already reported the feasibility and clinical potential of FDG PET for detecting and differentiating pancreatic carcinoma and reported that the threshold line of malignant or benign was SUV 2.2 (*9*). In clinical FDG PET, we sometimes experienced some malignant cases with low SUV and benign cases with high SUV, such as Patients 4 and 12 who were false-negative and Patient 36 who was false-positive in this study. Analysis of these difficult cases suggested that the difficult points for accurate clinical diagnosis of FDG PET might lie in tumor cell cellularity.

Higashi et al. (*14*) showed in their in vitro study that FDG accumulation has a close relationship with the number of viable tumor cells rather than the proliferative activity. Ito et al. (*19,20*) also suggested the significance of the cellularity in their clinical study. These studies support our clinical finding, but to evaluate the cellularity problem in the clinical field there were wide differences between in vivo and in vitro studies. Only concerning tumor characteristics, we had to evaluate, in our clinical PET study, several different kinds of histology, differentiation, amount of connective tissue, solid or cystic tumor type, GLUT-1 immunoreactivity and tumor size. To restrict and eliminate these influential conditions, there were three major problems to be solved concerning tumor size, counting method and histological differences.

First, we had to address the influence of tumor size. Our multivariate analysis results showed that tumor size and SUV did not have a significant relationship with each other. Ito et al. also reported similar results (*19,20*). If a tumor was smaller than 20 mm, partial volume effect could have a great influence on SUV. But in this study, we had only four cases with tumors under 20 mm in size. Even in larger-sized tumors, there was no

TABLE 3
Results of Tumor Cell Counting in Each GLUT-1 Grading

Patient no.	GLUT-1 negative cells			GLUT-1 positive cells						Total cells	
				Weak			Strong				
	Average	±s.d.	%	Average	±s.d.	%	Average	±s.d.	%	Average	±s.d.
1	17826	±6314	100.0	0	±0	0.0	0	±0	0.0	17826	±6314
2	18656	4099	100.0	0	0	0.0	0	0	0.0	18656	4099
3	40939	1453	100.0	0	0	0.0	0	0	0.0	40939	1453
4	6253	7136	38.9	9804	10424	61.1	0	0	0.0	16057	17548
5	22688	15721	36.2	39943	19062	63.8	0	0	0.0	62631	3407
6	9408	5998	41.2	15040	3257	65.9	0	0	0.0	22808	2480
7	362	241	3.2	11097	5195	96.8	0	0	0.0	11458	5192
8	60324	5481	84.0	11498	2555	16.0	0	0	0.0	71821	6102
9	0	0	0.0	8185	1413	100.0	0	0	0.0	8185	1413
10	0	0	0.0	27519	2035	100.0	0	0	0.0	27519	2035
11	0	0	0.0	12675	1120	100.0	0	0	0.0	12675	1120
12	0	0	0.0	0	0	0.0	3213	698	100.0	3213	698
13	3839	1592	9.3	21743	3049	52.4	15886	4346	38.3	41468	1977
14	0	0	0.0	0	0	0.0	5890	1724	100.0	5890	1724
15	0	0	0.0	6033	4610	34.7	11355	2913	65.3	17388	7232
16	1673	942	9.9	5673	1517	33.6	9523	1881	56.5	16869	2014
17	2224	1023	10.3	8765	2809	40.6	10589	4857	49.1	21578	6963
18	0	0	0.0	237	420	6.0	3687	564	94.0	3924	574
19	0	0	0.0	2548	934	34.3	4882	1312	65.7	7430	1494
20	0	0	0.0	0	0	0.0	8975	3256	100.0	8975	3256
21	0	0	0.0	0	0	0.0	12901	1342	100.0	12901	1342
22	0	0	0.0	0	0	0.0	15130	5380	100.0	15130	5380
23	0	0	0.0	0	0	0.0	24580	4229	100.0	24580	4229
24	46	58	0.5	1013	415	10.8	8360	1709	88.8	9418	1960
25	0	0	0.0	663	1326	2.7	23895	1794	97.3	24558	2221
26	13727	3083	25.8	20245	4407	38.0	19278	3937	36.2	53250	5967
27	0	0	0.0	4291	2572	24.6	13119	3923	75.4	17410	2134
28	0	0	0.0	2566	1520	19.2	10791	3051	80.8	13357	2756
29	0	0	0.0	0	0	0.0	14204	2769	100.0	14204	2769
30	452	304	7.9	666	245	11.7	4593	1957	80.4	5711	1688
31	0	0	0.0	0	0	0.0	31189	6437	100.0	31189	6437
32	0	0	0.0	4558	3497	12.4	32302	5182	87.6	36860	1750
33	724	734	0.9	10554	3887	12.5	72939	6393	86.6	84217	5814
34	0	0	0.0	698	168	66.7	347	103	33.2	1046	246
35	0	0	0.0	0	0	0.0	1597	527	100.0	1597	527
36	10303	7546	17.2	31529	25426	52.6	18165	11318	30.3	59996	17310

significant correlation. Why did larger-sized tumors have relatively larger SUVs? We believe that the heterogeneity of tumor cell cellularity was the main factor for this phenomenon. The ROI was placed over in area of tumor that showed the highest FDG activity, which means that the ROI could have the most dense population of tumor cells in it. If a tumor was large enough, it could have a wider range of heterogeneity of tumor cell cellularity. There could be many areas of dense tumor cell population. Our results of the relationship between tumor size and SUV also could be explained by the effect of tumor cell cellularity.

Second, tumor size also had a great influence on GLUT-1 immunohistochemical counting methods. In our previous article, the heterogeneity of the intratumoral distribution of GLUT expression was not considered (*13*). If a tumor had some strong staining among its tumor cells, the grade of GLUT immunoreactivity of the tumor was categorized as strong, independent from the distribution of GLUT-expressed cells. But, in fact, some tumors were stained strong positive all over the tumor area (Fig. 2A). Another tumor was stained strong positive in some areas and negative in another area on the same section (Fig. 2B, C). Another tumor had a great deal of cystic area or connective tissue (Fig. 2D). These heterogeneities were thought to increase in relation to tumor size and to affect the wide range of SUVs in the GLUT-1 strong group as well. In usual immunohistochemical examinations or the original counting method of Wang et al., tumor cell counting was performed only subjectively or in a small-sized area of less than 1 × 1 mm square (*23,25,26*). But in such a small area, the heterogeneity of GLUT-1 expression was thought to be neglected. In our tumor counting method, two restrictions were considered. The size of the counting area was defined as 5 × 5 mm square, as wide as possible to reach the size of the 10- × 10-mm ROI in an FDG PET study. Furthermore, the tissue sections were resected in the middle of the tumor area and were sufficiently larger than 1 cm in diameter of tumor tissue area. Under these conditions, the influence of GLUT-1 immunohistochemical heterogeneity and tumor size could be eliminated.

Third, in addressing histological differences in this study, we counted every tumor cell as one whatever the histology of the tumor cell was. Could we count a malignant tumor cell as one just the same as a benign tumor cell? Could we count a islet cell tumor cell just the same as a ductal adenocarcinoma cell that formed a malignant tubule? Table 2 clearly supported the correctness of our tumor cell counting method. There was a close relationship between SUVs and cellularity in each histological type, especially in malignant cases. Our previous article suggested that the neoplastic cellular character could have a

TABLE 4
Intra- and Interobserver Variance in Tumor Cell Counting: Analysis of Multiple Regression Coefficient of Determination

GLUT-1 grading	GLUT-1 negative cells				GLUT-1 positive cells: Weak				GLUT-1 positive cells: Strong				Total tumor cells			
	R-square				R-square				R-square				R-square			
Counting	Physician 1, count 1	Physician 1, count 2	Physician 2	Physician 3	Physician 1, count 1	Physician 1, count 2	Physician 2	Physician 3	Physician 1, count 1	Physician 1, count 2	Physician 2	Physician 3	Physician 1, count 1	Physician 1, count 2	Physician 2	Physician 3
Physician 1, count 1	//	0.998	0.789	0.913	//	0.966	0.452	0.69	//	0.995	0.894	0.958	//	0.992	0.849	0.904
Physician 1, count 2	0.998	//	0.791	0.919	0.966	//	0.445	0.731	0.995	//	0.9	0.969	0.992	//	0.9	0.969
Physician 2	0.789	0.791	//	0.769	0.452	0.445	//	0.314	0.894	0.9	//	0.93	0.849	0.9	//	0.93
Physician 3	0.913	0.919	0.769	//	0.69	0.731	0.314	//	0.958	0.969	0.93	//	0.904	0.969	0.93	//

// = not done.

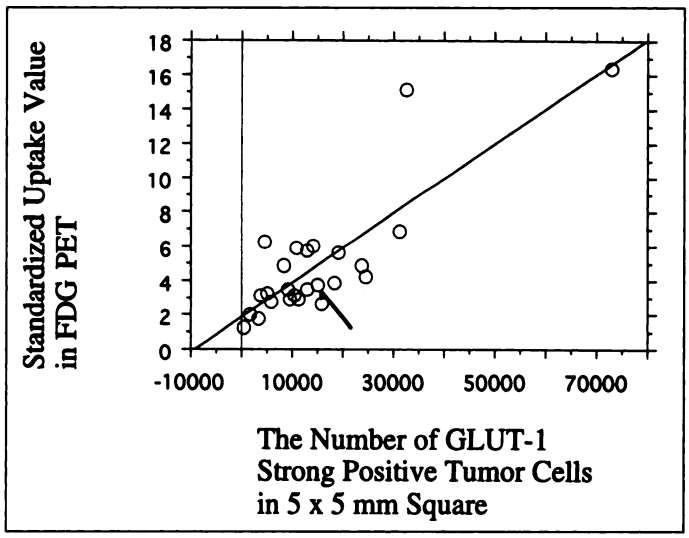

FIGURE 3. Comparison between standardized uptake values and number of GLUT-1 strong-positive tumor cells in a 5- × 5-mm square in resected section of 25 GLUT-1 strong-positive pancreatic tumor cases. There was significant correlation between them at $p < 0.005$. Arrow shows solid and cystic tumor in Patient 36.

closer relationship with FDG accumulation than the malignant potential of tumor cells (*13*). In this study, a solid and cystic tumor (Fig. 2E) was only one example but a good one. The malignant potential of this tumor is known to be low, but its FDG accumulation was known to be higher than with the usual benign tumors (*27*). This tumor had a huge number (59,996) of total cellularity, in spite of its cystic or necrotic component, but only about 30% of the tumor cells had strong immunoreactivity of GLUT-1. The relationship between SUV and the number of the GLUT-1 strong positive tumor cells of this tumor was just on the regression line (Fig. 3, arrow). This result could support our counting methods and our impression in the previous article. Concerning the malignant potential, those of islet cell tumors also have been the subject of considerable controversy. Porter et al. (*28*) pointed out that what may be the "pathologist's carcinoma" may not turn out to be the "patient's cancer." Consequently, it may be said in this study that a pancreas tumor could have a higher rate of entry of FDG if it had both higher tumor cell cellularity and increased expression of GLUT-1 transporter altogether, independent from its histology or malignant potential.

We can say that if a tumor had strong GLUT-1 immunoreactivity there was a significantly close relationship between GLUT-1 strong positive tumor cell cellularity and FDG accumulation in the clinical PET study, independent from the tumor size, the heterogeneity of intratumoral distribution of GLUT-1 expression, the histological type and the malignant potential of the tumor.

GLUT-1 expression was supposed to play an essential role in higher FDG accumulation. In other words, GLUT-1 might be only a precondition for higher FDG accumulation. GLUT-1 expression can be activated by not only malignant transformation of a cell (*29,30*) but also by the normal development and growth condition (*31*), whenever the higher increased glucose consumption was needed. These studies showed that the increase of GLUT-1 gene expression in response to oncogenes is likely mediated by similar or identical biochemical signaling pathways to the increase of GLUT-1 gene expression observed in response to growth factors during normal growth conditions. Therefore, in the view of tumor cells one by one, it is likely that a level of increased glucose consumption of each tumor cell, if it once becomes more than a certain level, may reach a plateau and may be almost all the same, independent from the character of the tumor as a tissue, such as the histological type and the malignant potential. The phrase "increased FDG accumulation," which was often used in the FDG PET study as a hackneyed expression for malignancy, may only mean the dense histological character of the tumor as a tissue.

Table 2 shows that ductal adenocarcinoma tumors had a narrow range of SUVs (from 2.52–6.9), and their standard deviations were very low despite their large numbers. The table also shows that the tumor cell cellularity had the same tendency. These results meant that there was a certain limitation of SUVs and cellularity in ductal adenocarcinoma tumors. The most likely explanation is the character of desmoplastic change of ductal adenocarcinoma. Most of them tend to have a great deal of fibrous stroma in their tissues (Fig. 5D). We say that, because of the desmoplastic change, ductal adenocarcinoma tumors could not have higher SUVs. A similar tendency of cystadenocarcinoma between their SUVs and the tumor cell cellularity also was revealed in Table 3, probably because of the cystic change. On the other hand, islet cell tumors, for example, have less tendency toward desmoplastic change, and their SUVs and cellularity were higher than those of ductal adenocarcinomas. The same was true of the solid and cystic tumor. Results of other kinds of tumors with lower desmoplastic change, such as malignant lymphomas, are needed for further confirmation.

We may reasonably conclude that an adequate knowledge and consideration of histology or cellularity of a tumor tissue is needed for accurate FDG PET diagnosis. It could be said that each threshold line of SUV from malignant to benign tumor must be different from every other histological type of the tumor.

The relationship between inflammation and increased FDG uptake was not discussed in this article. In the view of a tumor cell one by one, it is likely that the level of increased glucose consumption of each tumor cell may be almost the same. However, it is supposed that the level of glucose consumption of inflammatory cells is quite different from that of tumor cells.

TABLE 5
Results of Multiple Regression Analysis for Standardized Uptake Values

Variances	Analysis of 36 cases			Analysis of 34 cases		
	Beta	B	p	Beta	B	p
Number of GLUT-1 strong-positive tumor cells	0.854949	0.00019	0.0000723*	0.671004	0.00017	0.0028743*
Number of GLUT-1 positive tumor cells	0.115603	0.00002	0.6587809	0.524335	0.0001	0.1561657
Number of total tumor cells	−0.12984	−0.00002	0.5212448	−0.580596	−0.00009	0.0989214
GLUT-1 grading	−0.227172	−1.1009	0.101209	−0.442227	−1.64563	0.0528174
Tumor size (mm)	0.175356	0.02642	0.0931451	0.272006	0.03102	0.0621477

Beta = standard regression coefficient; B = regression coefficient.

In the immunohistochemistry, there were several inflammatory pseudotumor cases with various types of GLUT-1 immunoreactivity, but it was difficult to have a quantitative comparison with malignant tumor cases. In this article, we eliminated some inflammatory pseudotumor cases. Further study is needed.

CONCLUSION

In pancreatic FDG PET imaging, a high degree of both GLUT-1 expression and tumor cell cellularity is needed for a pancreatic tumor to have a higher FDG accumulation. GLUT-1 expression was supposed to play an essential role in higher FDG accumulation. Only in the condition of GLUT-1 strong positive expression was the cellularity supposed to have a significant effect on SUVs.

ACKNOWLEDGMENTS

We thank Dr. Yasuhiro Magata, Dr. Satoshi Sasayama and Haruhiro Kitano of the Department of Nuclear Medicine, Kyoto University Faculty of Medicine, for technical assistance with PET imaging.

REFERENCES

1. Bares R, Klever P, Hauptmann S, et al. F-18 fluorodeoxyglucose PET in vivo evaluation of pancreatic glucose metabolism for detection of pancreatic cancer. *Radiology* 1994;192:79–86.
2. Hawkins RA, Hoh C, Dahlbom M, et al. PET cancer evaluations with FDG [Editorial]. *J Nucl Med* 1991;32:1555–1558.
3. Ishizu K, Sadato N, Yonekura Y, et al. Enhanced detection of brain tumors by [18F]fluorodeoxyglucose PET with glucose loading. *J Comput Assist Tomogr* 1994; 18:12–15.
4. Kern KA, Brunetti A, Norton JA, et al. Metabolic imaging of human extremity musculoskeletal tumors by PET. *J Nucl Med* 1988;29:181–186.
5. Kubota K, Matsuzawa T, Fujiwara T, et al. Differential diagnosis of lung tumor with positron emission tomography: a prospective study. *J Nucl Med* 1990;31:1927–1932.
6. Strauss LG, Clorius JH, Schlag P, et al. Recurrence of colorectal tumors: PET evaluation. *Radiology* 1989;170:329–332.
7. Torizuka T, Tamaki N, Inokuma T, et al. Value of fluorine-18-FDG-PET to monitor hepatocellular carcinoma after interventional therapy. *J Nucl Med* 1994;35:1965–1969.
8. Wahl RL, Cody RL, Hutchins GD, Mudgett EE. Primary and metastatic breast carcinoma: initial clinical evaluation with PET with the radiolabeled glucose analogue 2-[F-18]-fluoro-2-deoxy-D-glucose. *Radiology* 1991;179:765–770.
9. Inokuma T, Tamaki N, Torizuka T, et al. Evaluation of pancreatic tumors with positron emission tomography and F-18 fluorodeoxyglucose: comparison with CT and US. *Radiology* 1995;195:345–352.
10. Inokuma T, Tamaki N, Torizuka T, et al. Value of fluorine-18-fluorodeoxyglucose and thallium-201 in the detection of pancreatic cancer. *J Nucl Med* 1995;36:229–235.
11. Yonekura Y, Benua RS, Brill AB, et al. Increased accumulation of 2-deoxy-2-[18F]fluoro-D-glucose in liver metastases from colon carcinoma. *J Nucl Med* 1982; 23:1133–1137.
12. Warburg O. The metabolism of tumors. *Constable* 1930:254–270.
13. Higashi T, Tamaki N, Honda T, et al. Expression of glucose transporters in human pancreatic tumors compared with increased FDG accumulation in PET study. *J Nucl Med* 1997;38:1337–1344.
14. Higashi K, Clavo AC, Wahl RL. Does FDG uptake measure proliferative activity of human cancer cells? In vitro comparison with DNA flow cytometry and tritiated thymidine uptake *J Nucl Med* 1993;34:414–419.
15. Torizuka T, Tamaki N, Inokuma T, et al. In vivo assessment of glucose metabolism in hepatocellular carcinoma with FDG-PET. *J Nucl Med* 1995;36:1811–1817.
16. Wahl RL. Targeting glucose transporters for tumor imaging: "sweet" idea, "sour" results. *J Nucl Med* 1996;37:1038–1041.
17. Brown RS, Leung JY, Fisher SJ, Frey KA, Ethier SP, Wahl RL. Are inflammatory cells important? *J Nucl Med* 1995;36:1854–1861.
18. Kubota K, Yamada S, Kubota K, et al. Intratumoral distribution of fluorine-18-fluorodeoxyglucose in vivo: high accumulation in macrophages and granulation tissues studied by microautoradiography. *J Nucl Med* 1992;33:1972–1980.
19. Ito K, Kato T, Ohta M, et al. Diagnositc usefulness and limitation of FDG-PET in recurrent rectal cancer. In: Matsuzawa T, ed. *Proceedings of the second international symposium of clinical PET in oncology.* Singapore: World Scientific; 1994:199–206.
20. Kato T, Fukatsu H, Ito K, et al. Fluorodeoxyglucose positron emission tomography in pancreatic cancer: unsolved problem. *Eur J Nucl Med* 1995;22:32–39.
21. Tamaki N, Yonekura Y, Yamashita K, et al. Relation of left ventricular perfusion and wall motion with metabolic activity in persistent defects on thallium-201 tomography healed myocardial infarction. *Am J Cardiol* 1988;62:202–208.
22. Woodard HQ, Bigler RE, Freed B. Expression of tissue isotope distribution [Letter]. *J Nucl Med* 1975;16:958–959.
23. Wang LD, Shi ST, Zhou Q, et al. Changes in p53 and cyclin D1 protein levels and cell proliferation in different stages of human esophageal and gastric-cardia carcinogenesis. *Int J Cancer* 1994;59:514–519.
24. Cooley WW, Lohnes PR. *Multivariate data analysis.* New York: John Wiley and Sons; 1971.
25. Wang ZH, Manabe T, Ohshio G, et al. Immunohistochemical study of heparan sulfate proteoglycan in adenocarcinomas of the pancreas. *Pancreas* 1994;9:758–763.
26. Ohshio G, Yoshioka H, Manabe T, et al. Expression of sialosyl-Tn antigen (monoclonal antibody MLS102 reactive) in normal tissues and malignant tumors of the digestive tract. *J Cancer Res Clin Oncol* 1994;120:325–330.
27. Okazumi S, Enomoto K, Fukunaga T, et al. Evaluation of pancreatic lesions using 18F-fluorodeoxyglucose PET. *J Japan Pancreas Society* 1994;9:155–160.
28. Porter MR and Frantz VK. Tumors associated with hypoglycemia: pancreatic and extrapancreatic. *Am J Med* 1956;21:944.
29. Merrall NW, Plevin R, Gould GW. Growth factors, mitogens, oncogenes and the regulation of glucose transport. *Cell Signal* 1993;5:667–675.
30. Birnbaum MJ, Haspel HC, Rosen OM. Transformation of rat fibroblasts by FSV rapidly increases glucose transporter gene transcription. *Science* 1987;235:1495–1498.
31. Dermietzel R, Krause D, Kremer M, Wang C, Stevenson B. Pattern of glucose transporter (Glut 1) expression in embryonic brains is related to maturation of blood-brain barrier tightness. *Dev Dyn* 1992;193:152–163.
32. Hermanek P, Sobin LH. *TNM classification of malignant tumors*, 4th ed. New York: Springer-Verlag; 1987.